

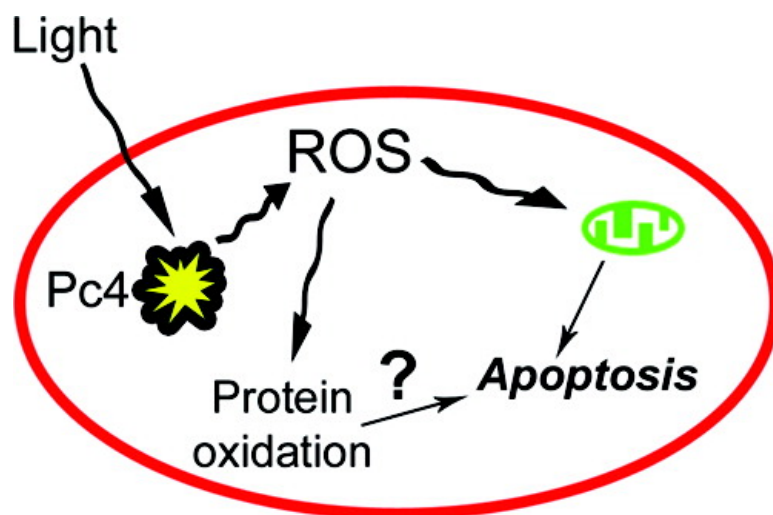
Article

## Immediate Protein Targets of Photodynamic Treatment in Carcinoma Cells

Pavel A. Tsaytler, Martina C. O'Flaherty, Dmitri V. Sakharov, Jeroen Krijgsveld, and Maarten R. Egmond

*J. Proteome Res.*, 2008, 7 (9), 3868-3878 • DOI: 10.1021/pr800189q • Publication Date (Web): 25 July 2008

Downloaded from <http://pubs.acs.org> on November 28, 2008



### More About This Article

Additional resources and features associated with this article are available within the HTML version:

- Supporting Information
- Access to high resolution figures
- Links to articles and content related to this article
- Copyright permission to reproduce figures and/or text from this article

[View the Full Text HTML](#)

## Immediate Protein Targets of Photodynamic Treatment in Carcinoma Cells

Pavel A. Tsaytler,<sup>†</sup> Martina C. O'Flaherty,<sup>‡</sup> Dmitri V. Sakharov,<sup>†</sup> Jeroen Krijgsveld,<sup>‡</sup> and Maarten R. Egmond<sup>\*†</sup>

Department of Membrane Enzymology, Bijvoet Center for Biomolecular Research, Utrecht University, Padualaan 8, Utrecht 3584 CH, The Netherlands, and Biomolecular Mass Spectrometry and Proteomics Group, Bijvoet Center for Biomolecular Research and Utrecht Institute for Pharmaceutical Sciences, Utrecht University, Sorbonnelaan 16, Utrecht 3584 CA, The Netherlands

Received March 13, 2008

Oxidative stress induced in tumor cells undergoing photodynamic treatment (PDT) leads to extensive modification of many proteins in these cells. Protein oxidation mainly gives rise to formation of carbonyls and oxidized thiols. The immediate targets of PDT-induced protein oxidation in A431 tumor cells have been identified using a proteomic approach involving selective biotinylation, affinity purification and mass spectrometric identification of modified proteins. In all, 314 proteins were shown to undergo PDT-mediated oxidative modifications. While abundant structural proteins and chaperones represented a significant fraction of the carbonylated proteins, labeling of proteins containing oxidized thiols allowed identification of many proteins at low abundance and those involved in signaling and redox homeostasis. On the basis of the identification of these proteins, several likely mechanisms of PDT-induced triggering of apoptosis were put forward. This may not only lead to a further understanding of the complex network of cellular responses to oxidative stress, but it may also help in detailed targeting of photodynamic treatment applied to cancer.

**Keywords:** photodynamic treatment • protein • oxidation • carbonylation • thiol • cysteine • biotinylation • identification

### Introduction

Photodynamic therapy is a promising treatment of neoplastic and nonneoplastic diseases. It is currently being used in the treatment of many cancers including lung, prostate, head and neck cancers. It is based on the concept that certain light-sensitive compounds (photosensitizers) can be preferentially localized in tumor tissue and become activated by light with an appropriate wavelength to generate free radicals and singlet (<sup>1</sup>Δ<sub>g</sub>) oxygen. These reactive oxygen species (ROS) will lead to damage of cellular components in close proximity to the photosensitizer and eventually give rise to tumor cell death either by necrosis or apoptosis.<sup>1</sup> The cellular responses to photodynamic treatment (PDT) have been extensively studied *in vitro* during the last decades using various types of cells and photosensitizers, as has been reviewed recently.<sup>2–4</sup> Depending on the cell type, subcellular localization and the nature of photosensitizer, PDT has been shown to activate numerous signaling pathways that sometimes play controversial roles. The diversity of models and cellular responses makes it challenging to pinpoint the main early events involved in apoptotic death. Moreover, most of the studies of PDT-mediated apoptosis have been focused on the late apoptotic events, rather than immediate cellular responses to PDT that trigger apoptotic pathways. Know-

ing the molecular mechanisms of triggering and propagation of PDT-induced apoptosis may lead to improvement of the therapeutic efficiency of photodynamic therapy.

Oxidative modifications of proteins represent one of the cellular effects of PDT. Oxidative modifications, particularly thiol oxidation and carbonylation, have been shown to modify protein activity either reversibly or irreversibly by altering enzymatic function or by disturbing protein–protein interactions.<sup>5–7</sup> In a recent study, a specific set of proteins, including molecular chaperones and structural proteins, have been found to become carbonylated in response to oxidative stress induced by PDT.<sup>8</sup> Their findings conform to the concept that oxidative damage of the proteins induced by oxidative stress is selective and that proteins with specific sensitivity to oxidation can regulate cellular signaling events, including apoptosis. However, it is known that the cellular responses to PDT depend on the cell type, the nature of the photosensitizer, and the treatment conditions. Therefore, any hypothesis of the selectivity of PDT-induced protein oxidation needs to be verified by studying it in different systems. Additionally, although some redox-sensitive proteins have clearly been shown to operate in the processes regulating apoptosis,<sup>9,10</sup> the significance of PDT-induced oxidative modifications of proteins for the triggering and progression of apoptosis remains obscure.

To date, determination of specific protein targets triggering PDT-mediated apoptosis has been a challenging and unresolved task. The aim of the present paper was to identify proteins that undergo oxidative modifications in immediate

\* To whom correspondence should be addressed. E-mail, m.r.egmond@uu.nl; tel., +3130-253-3526.

<sup>†</sup> Department of Membrane Enzymology.

<sup>‡</sup> Biomolecular Mass Spectrometry and Proteomics Group.

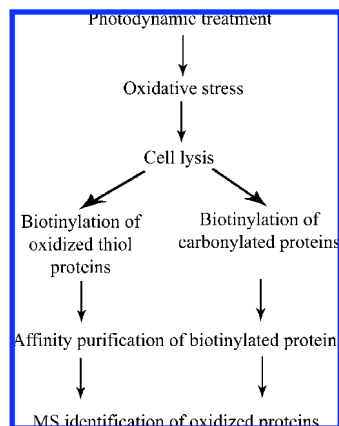


**Figure 1.** Schematic representation of the comprehensive proteomic approach for identification of PDT-induced oxidatively modified proteins. Two different types of protein oxidative modifications (oxidation of thiols and carbonylation) can be detected and identified using this approach.

response to oxidative stress induced by PDT. For our investigation, we used human epidermoid carcinoma cells A431 exposed to Pc4, an active phthalocyanine photosensitizer, which currently is in Phase I clinical trials.<sup>11</sup> To achieve our goal, we performed a proteomic analysis, comprising detection and identification of two types of oxidative protein modifications, carbonylation and thiol oxidation. Thus, this study represents the first application of highly sensitive proteomic approach for identification of both types of protein oxidation in the same system (Figure 1). Oxidative site-specific biotinylation allowed purification of oxidatively modified proteins, followed by mass spectrometric identification. In A431 cells, 314 proteins were found to be oxidized upon treatment with Pc4. These included both abundant species, such as structural proteins, chaperones, and energy metabolism enzymes, as well as low-abundance signaling proteins, involved in the regulation of proliferation and apoptosis. Several proteins, identified in our research, were selected and their role in PDT-mediated triggering of apoptosis was discussed.

## Experimental Section

**Materials.** The phthalocyanine photosensitizer Pc4 [HOSiPcOSi(CH<sub>3</sub>)<sub>2</sub>(CH<sub>2</sub>)<sub>3</sub>N(CH<sub>3</sub>)<sub>2</sub>] was provided by Nancy L. Oleinick (Department Radiation Oncology, Case Western Reserve University, Cleveland, OH). Stock solution (1 mM) of Pc4 in DMF was prepared and stored at -80 °C. Micro Bio-Spin 6 chromatography columns were from Bio-Rad Laboratories (Hercules, CA); protease inhibitors cocktail was from Sigma; Hoechst 33342 stain was from Invitrogen; maleimide-PEO2-biotin was from Pierce.

**Cell Culture.** The human epidermoid carcinoma cells A431 were cultured in Dulbecco's Modified Eagle Medium (DMEM) supplemented with 10% fetal bovine serum, penicillin (100 units/mL), streptomycin (100 µg/mL), and amphotericin B (0.25 µg/mL) in 5% CO<sub>2</sub>, 95% air at 37 °C in a humidified incubator. In all experiments 75–85% confluent cells were used.

**Photodynamic Treatment.** Cells were incubated with photosensitizer Pc4 in complete culture medium for 3 h at 37 °C. The medium containing photosensitizer was replaced with PBS supplemented with 0.9 mM CaCl<sub>2</sub>, 0.5 mM MgCl<sub>2</sub>, and 5 mM glucose (PBS+), and cells were irradiated for 3 min with visible

light from a slide projector to a final fluence of 0.9 J/cm<sup>2</sup>. After illumination, PBS+ was aspirated; cells were washed with PBS and processed as desired. All manipulations with cells and lysates were carried out in the dark. The dark control samples were processed using the exact same procedure, except irradiation was omitted.

**Estimation of Apoptosis Caused by PDT.** The efficacy of PDT to induce apoptotic death of A431 cells was assessed by detection of the product of poly(ADP-ribose) polymerase (PARP) cleavage. Cells subjected to PDT with Pc4 were incubated in complete DMEM for 2 h at 37 °C and lysed in lysis buffer A (40 mM Hepes, 50 mM NaCl, 1 mM EDTA, 1 mM EGTA, pH 7.4, 1% CHAPS, and protease inhibitors). Lysates were centrifuged at 20 000g for 15 min and supernatants were collected. Total protein concentration was measured by using the Bio-Rad protein assay. Proteins were separated on 10% SDS-PAGE and transferred onto nitrocellulose membrane. PARP (cleaved and noncleaved) was detected with primary polyclonal anti-PARP antibody and secondary anti-rabbit IgG conjugated to HRP (both from Santa Cruz Biotechnology) using the ECL detection system (Amersham Pharmacia Biotech). Alternatively, cells were incubated for 10 min with 1 µg/mL Hoechst solution in PBS to stain nuclei and assessed for typical apoptotic morphology (nuclear condensation and fragmentation) using a Nikon Eclipse TE2000-U fluorescence microscope. To estimate the apoptotic response, apoptotic and total cell numbers were counted in several random areas of PDT-treated cells, followed by calculation of the apoptotic to total cell number ratios.

**Biotinylation of Carbonylated Cellular Proteins.** Cells subjected to PDT were washed with PBS and lysed in lysis buffer A (1 mL/100 cm<sup>2</sup> of 80% confluent cells). Lysates were centrifuged at 20 000g for 15 min. After collection of supernatants, biotinylation was accomplished as reported previously,<sup>12</sup> with some modifications: 1 vol of lysate was gel-filtrated with Sephadex G-25 in biotinylation buffer (100 mM sodium phosphate, 150 mM NaCl, pH 7.2), followed by addition of 4 vol of 6.25 mM biotin hydrazide in the same buffer and 2 h incubation at room temperature. Vessels containing reactive mixture were transferred on ice and 5 vol of 30 mM NaCNBH<sub>3</sub> in biotinylation buffer was added. Upon 30 min incubation, samples were gel-filtrated with Sephadex G-25 in biotinylation buffer and frozen at -80 °C.

**Biotinylation of Reversibly Oxidized Thiol Proteins.** Cells subjected to PDT were washed with PBS, followed by addition of lysis buffer A containing 50 mM *N*-ethylmaleimide (NEM), 15 min incubation on ice, collection, and centrifugation of the lysates at 20 000g for 15 min. Lysates were gel-filtrated with Sephadex G-25 in PBS, and DTT was added to 1 mM final concentration. After 10 min incubation at room temperature, biotin maleimide was added to 1.5 mM. The mixture was incubated for 1 h, gel-filtrated with Sephadex G-25 in PBS, and frozen at -80 °C.

To induce extensive protein thiols oxidation, for validation of the labeling protocol, cells were incubated with the indicated concentration of diamide in PBS for 10 min at 37 °C, washed with PBS, and processed as described above.

**Affinity Purification of Oxidatively Modified Proteins.** After biotinylation, oxidized proteins were purified by affinity chromatography with neutravidin agarose. Samples containing 0.1% SDS were incubated with 10% (v/v) of neutravidin agarose beads overnight at 4 °C. After washing of the beads four times with 50 mM Tris, 8 M urea, and 200 mM NaCl, pH 8, and twice

with PBS, proteins were eluted with 2-fold PAGE loading buffer and separated on 10% SDS-PAGE, followed by silver staining.

**Gel Destaining and In-Gel Digestion.** Each lane from silver-stained gel was cut into 20 slices of equal size. Each slice was cut into small cubes prior to digestion. The gel pieces were placed in a 0.5-mL tube, washed with 250  $\mu$ L of water and destained with 100  $\mu$ L of 30 mM  $K_3Fe(CN)_6$ , 100 mM  $Na_2S_2O_3$  in water. The samples were washed with 250  $\mu$ L of water, followed by 15 min dehydration with 100% acetonitrile (ACN). Proteins were reduced with 100  $\mu$ L of 10 mM DTT in 50 mM  $NH_4HCO_3$  for 1 h at 60  $^{\circ}C$ , followed by dehydration with 100% ACN and incubation in 100  $\mu$ L of 55 mM iodoacetamide in 50 mM  $NH_4HCO_3$  in the dark. Then the gel pieces were dehydrated twice with 100  $\mu$ L of 100% ACN, and 20  $\mu$ L of 12 mg/mL trypsin in 50 mM  $NH_4HCO_3$  was added to each sample, followed by 30 min incubation at 4  $^{\circ}C$ . Upon removing the excess of trypsin, samples were incubated in 20  $\mu$ L of 50 mM  $NH_4HCO_3$  overnight at 37  $^{\circ}C$ , and the supernatants were transferred to new tubes. Peptides were extracted from the gel pieces with 5% formic acid for 2 min at 65  $^{\circ}C$ , followed by shaking for 20 min. Supernatants were collected and combined with the ones from the previous step.

**LC-LTQ Mass Spectrometry Analysis.** Nanoscale liquid chromatography MS/MS was performed by coupling an Agilent 1100 Series LC system with a LTQ quadrupole ion trap mass spectrometer (Finnigan, San Jose, CA). Peptide mixtures were concentrated and desalted using an online C18 trap column (o.d. 375  $\mu$ m, i.d. 100  $\mu$ m packed with 20 mm of 5  $\mu$ m AQUA C<sub>18</sub>, RP particles (Phenomenex)) and further separation was achieved by gradient elution of peptides onto a C18 reverse phase column (o.d. 375  $\mu$ m, i.d. 50  $\mu$ m packed with 15 cm of 3  $\mu$ m C<sub>18</sub>, RP particles (Reprosil)). MS detection in the LTQ was achieved by directly spraying the column eluent into the electrospray ionization source of the mass spectrometer via a butt-connected nanoelectrospray ionization emitter (New Objective). A linear 60 min gradient (10–45% B) was applied for peptide elution into the MS at a final flow rate of 100 nL/min. The total analysis time was 1 h. Mobile phase buffers were 0.1 M acetic acid; 80% ACN, 0.1 M acetic acid.

The LTQ was operated in positive ion mode, and peptides were fragmented in data-dependent mode. One mass spectrometry survey zoom scan was followed by three data-dependent MS/MS scans. Target ions already selected for MS/MS were dynamically excluded for 30s.

**Database Searches.** Tandem mass spectra were extracted and charge state deconvoluted by BioWorks version 3.3. All MS/MS samples were analyzed using Mascot (Matrix Science, London, U.K.; version 2.1.02). Mascot was set up to search the fragment mass spectra against IPI\_HUMAN\_v3.36 database. The database was searched with a parent ion tolerance of 0.5 Da and a fragment ion mass tolerance of 0.9 Da. Fixed and variable modifications were the iodoacetamide derivative of cysteine and oxidation of methionine, respectively. Probability assessment of peptide assignments and protein identifications was made using Scaffold (version Scaffold-1.6, Proteome Software, Inc., Portland, OR). Only peptides with  $\geq 90\%$  probability were considered. Criteria for protein identification included detection of at least 3 unique identified peptides and a probability score of  $\geq 99\%$ .

## Results

**Apoptosis Induction by PDT.** To detect the PARP cleavage product formed within 2 h after PDT, lysates were applied

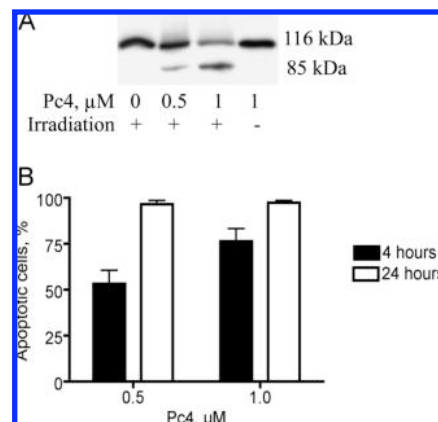


**Figure 2.** (A) Effect of photosensitizer Pc4 concentration on PDT-induced PARP cleavage in A431 cells. Western blotting detection with antibody to PARP. The 116 kDa bands correspond to full-length PARP, whereas 85 kDa bands correspond to the products of PARP cleavage and indicate apoptosis. (B) Percentage of apoptotic cells measured in 4 and 24 h after irradiation. Apoptosis was assessed by detection of condensed and fragmented Hoechst-stained nuclei.

to SDS-PAGE, blotted on nitrocellulose membrane, and PARP was detected with an antibody. Figure 2A shows the Pc4 concentration-dependent induction of PARP cleavage, demonstrating that PDT triggers apoptosis in A431 cells under our conditions (each figure reported in this paper is a representative of at least three biological repetitions of the experiment). Concentrations of Pc4 higher than 1  $\mu$ M were found to evoke necrotic cell death. Figure 2B shows the percentage of cells that undergo apoptosis in 4 and 24 h after irradiation. Whereas no apoptotic cells were detected in the control samples (no Pc4 or no irradiation, not shown), about 55 and 75% of A431 cells were undergoing apoptotic death in 4 h after PDT with 0.5 and 1  $\mu$ M Pc4, respectively. All cells were dead by apoptosis in 24 h after PDT with either 0.5 or 1  $\mu$ M Pc4.

**Biotin Hydrazide Labeling of Carbonylated Cellular Proteins.** The approach used in our study combines recently developed techniques for biotinylation of reversibly oxidized cysteines<sup>13</sup> and for selective labeling of protein carbonyls with biotin hydrazide.<sup>12,14–16</sup> Following photodynamic treatment, cells were immediately lysed and protein carbonyl groups were biotinylated by the reaction with biotin hydrazide. Figure 3 summarizes the results of these experiments. As compared to 0.5  $\mu$ M Pc4 (Figure 3A, lane 2), a further increase of concentration of Pc4 to 1  $\mu$ M (Figure 3A, lane 3) evokes more intense protein labeling and appearance of additional bands. At least two distinct bands were detected in the control sample without photosensitizer (Figure 3A, lane 1), indicating the presence of protein carbonyls in the intact cells. A slight increase in protein labeling in the dark control sample (Figure 3A, lane 4) was due to the inability to completely prevent the samples from daylight illumination during preparative steps. However, a clear difference in the amounts and intensities of the protein bands between lanes 3 and 4 in Figure 3A demonstrates that the observed protein oxidation reflects the effect of photodynamic treatment of A431 cells in vivo, rather than oxidation during lysates preparation and labeling. Prior to affinity purification, small portions of biotinylated samples were separated on SDS-PAGE, and the gel was stained with Coomassie Blue (Figure

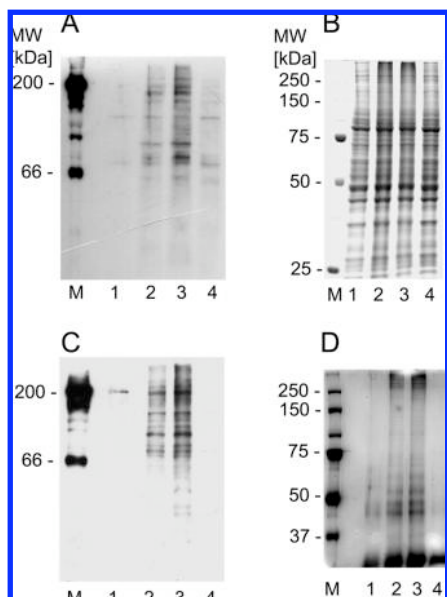


**Figure 3.** Photodynamic treatment of A431 cells with Pc4 results in increased protein carbonylation and subsequent labeling with biotin hydrazide. (A) PDT-induced oxidized biotinylated proteins detected on the Western blotting by neutravidin-HRP. (B) Coomassie staining of the same samples as in (A) separated on 10% SDS-PAGE gel. (C) Neutravidin agarose affinity purified oxidized biotinylated proteins detected on the Western blotting by neutravidin-HRP. (D) Silver staining of affinity purified oxidized biotinylated proteins separated on 10% SDS-PAGE. Lane M, biotinylated MW Standards (A and C); prestained MW Standards (Bio-Rad) (B and D). Lane 1, Pc4 0  $\mu$ M. Lane 2, Pc4 0.5  $\mu$ M. Lane 3, Pc4 1  $\mu$ M. Lane 4, Pc4 1  $\mu$ M without irradiation (dark control).

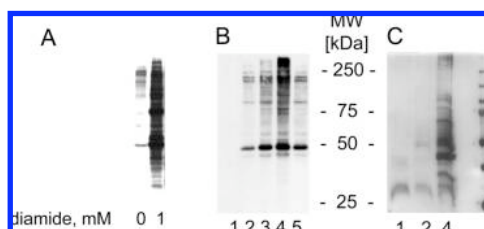


**Figure 4.** Labeling and affinity purification of oxidized thiol proteins. (A) A431 cells subjected to 1 mM diamide treatment undergo extensive protein thiol oxidation as shown by labeling with biotin maleimide and detection with neutravidin-HRP on the Western blot. (B) Western blotting detection of PDT-induced protein thiol oxidation. (C) Oxidized thiol proteins, affinity purified with neutravidin agarose for MS identification, were separated on 10% SDS-PAGE and visualized by silver staining. Lane 1, Pc4 1  $\mu$ M, no biotin maleimide labeling. Lane 2, Pc4 0  $\mu$ M. Lane 3, Pc4 0.5  $\mu$ M. Lane 4, Pc4 1  $\mu$ M. Lane 5, Pc4 1  $\mu$ M without irradiation (dark control).

3B). No significant difference in the amounts of proteins between samples was detected. The dark background and additional bands in the high molecular weight regions of the oxidized samples (Figure 3B, lanes 2, 3) resulted from PDT-induced protein cross-linking.

**Biotin Maleimide Labeling of Reversibly Oxidized Thiol Proteins.** Diamide, a compound that causes rapid and extensive oxidation of protein cysteines,<sup>17</sup> was used to validate the labeling procedure. Figure 4A shows that treatment of A431 cells with 1 mM diamide causes a dramatic

increase in the extent of biotinylation as compared to the control sample without diamide, indicating that the labeling strategy is effective and specific to oxidized thiols. Notably, this technique allows labeling of reversibly oxidized thiols only (e.g., sulfenic acid, intramolecular disulfides, mixed disulfides), whereas irreversible modifications (e.g., sulfinic or sulfonic acid, alkylation by lipid peroxidation products) will not be labeled. To determine optimal labeling conditions concentrations of DTT were varied, while biotin maleimide was fixed at 1.5 mM. Since 1 mM DTT resulted in intense labeling of oxidized samples and weak labeling of nonoxidized negative controls, it allowed us to study specifically PDT-oxidized proteins. Above 1 mM DTT labeling of PDT-oxidized proteins becomes very weak, while below 1 mM DTT, the difference in labeling between oxidized and nonoxidized proteins becomes less clear.

As was detected by Western blotting with neutravidin-HRP, PDT caused a Pc4-dependent increase in protein thiol oxidation (Figure 4B). While only few thiol proteins were labeled with biotin maleimide in the control sample without photosensitizer (Figure 4B, lane 2), PDT caused a significant increase in the intensities of these protein bands, together with the appearance of a large number of additional protein bands (Figure 4B, lanes 3, 4). No protein bands were detected in the control sample processed using the same labeling procedure lacking biotin maleimide (Figure 4B, lane 1), showing that the level of labeled proteins is much higher than that of naturally biotinylated proteins.

As in the case of biotin hydrazide labeled samples (Figure 3B), when biotin maleimide labeled proteins were separated on SDS-PAGE, followed by Coomassie staining, no differences in the amounts of proteins were detected, except for the formation of high molecular weight protein cross-links (data not shown).

**Affinity Purification and Identification of Oxidatively Modified Proteins by Mass Spectrometry.** After labeling of oxidatively modified proteins with either biotin hydrazide or biotin maleimide, they were affinity separated from other cellular proteins by overnight incubation with immobilized neutravidin agarose. Then agarose beads were extensively washed, followed by elution of biotinylated proteins with 2-fold PAGE loading buffer and their separation on SDS-PAGE.

Carbonylated proteins, labeled with biotin hydrazide and purified by affinity chromatography, were visualized by silver staining of the gel (Figure 3D). The same samples were separated on SDS-PAGE, transferred to the nitrocellulose membrane and detected by ECL with neutravidin-HRP (Figure 3C). Similar protein patterns on the Western blots before and after affinity purification (Figure 3, panels A and C, respectively) prove the enrichment of only carbonylated proteins labeled with biotin hydrazide. Interestingly, patterns of the same affinity-purified proteins visualized by Western blotting (Figure 3C) and by silver staining of SDS-PAGE (Figure 3D) were different. This observation demonstrates that there is no direct correlation between the amounts of purified oxidatively modified proteins and the extent of their oxidation and labeling. Thus, proteins within the molecular weight region from 70 to 200 kDa tend to be more heavily oxidized and labeled, whereas those with the molecular weight lower than 70 kDa tend to carry fewer carbonyl groups per protein (Figure 3, panels C and D).

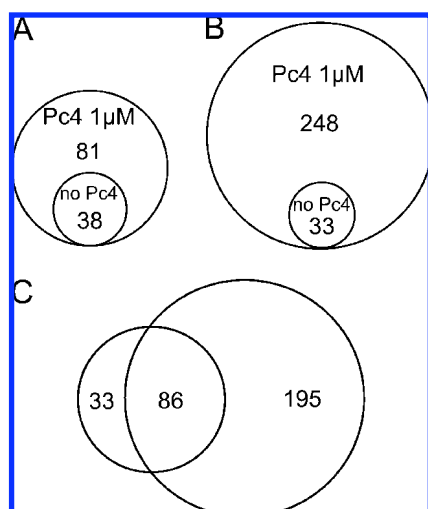


**Figure 5.** (A) Representation of the numbers of PDT-induced ( $1 \mu\text{M}$  Pc4) and naturally carbonylated (no Pc4) proteins in A431 cells. (B) Representation of the numbers of PDT-induced ( $1 \mu\text{M}$  Pc4) and naturally oxidized thiol proteins (no Pc4) in A431 cells. (C) Representation of the interrelation between PDT-induced carbonylated and oxidized thiol proteins. Of 314 oxidized proteins, 195 undergo only oxidation of thiols, 33 undergo only carbonylation, and 86 proteins contain both oxidative modifications.

Oxidatively modified thiol proteins labeled with biotin maleimide were affinity purified exactly as described for carbonylated proteins. Figure 4C shows purified oxidized thiol proteins separated on SDS-PAGE and visualized by silver staining. When affinity purified samples were blotted onto the nitrocellulose membrane and visualized by ECL with neutravidin-HRP (data not shown), the same protein patterns were detected as before affinity purification (Figure 4B), indicating that exactly the same oxidized thiol proteins labeled with biotin maleimide were enriched by affinity chromatography.

Upon affinity purification, proteins were identified by mass spectrometry. Since PDT with  $1 \mu\text{M}$  Pc4 induces apoptosis stronger than for  $0.5 \mu\text{M}$  Pc4 (Figure 2A) resulting in more intense protein oxidation (Figures 3A and 4B), only samples treated with 0 and  $1 \mu\text{M}$  Pc4 were chosen for MS identification. Affinity purified proteins were first separated on the SDS-PAGE. Two affinity purified control samples processed under exactly the same labeling procedures but lacking biotin maleimide and biotin hydrazide were also applied to the gel. The gel was then silver-stained and each lane was cut into 20 slices, followed by trypsinization. Peptide mixtures were applied on the LTQ mass spectrometer and obtained tandem mass spectra were analyzed using Mascot and Scaffold.

Proteins found in the control samples not labeled with biotin hydrazide or biotin maleimide were considered as an unspecific background and were excluded from the total list of proteins identified in all samples. Thus, 314 proteins were identified, including 119 carbonylated proteins, labeled with biotin hydrazide, and 281 proteins carried oxidatively modified cysteines, labeled with biotin maleimide. Of the 119 proteins identified after biotin hydrazide labeling, 38 were also found in the negative control not treated with Pc4 (Figure 5A). Most likely these are naturally carbonylated proteins. Similarly, of the 281 proteins identified after

labeling of oxidized thiols, 33 were identified in the negative control (Figure 5B). These are the proteins that upon physiological conditions contain either disulfide bridges, accessible for reduction with DTT, or other forms of oxidized cysteines, for example, glutathionylated proteins. Notably, oxidation of most of the proteins identified in negative controls significantly increased after  $1 \mu\text{M}$  Pc4 treatment, as follows from the numbers of peptides identified by MS/MS.<sup>18</sup> A Supplemental Table contains all identified carbonylated and oxidized thiol proteins from A431 cells subjected to PDT with either 0 or  $1 \mu\text{M}$  Pc4.

Comparison between  $1 \mu\text{M}$  Pc4 PDT-induced carbonylated and oxidized thiol proteins identified in A431 cells shows that 86 proteins undergo both types of oxidation (Figure 5C). Thus, 86 out of 119 carbonylated proteins also carry one or more oxidatively modified cysteines. This remarkably large overlap between these two independent experiments indicates the oxidation of specific classes of proteins, as well as the selectivity of our approach to capture these proteins.

Functional classification of all 314 identified proteins is shown in Figure 6A. Proteins involved in energy metabolism were separated from other metabolic enzymes, the biggest class of proteins oxidized by PDT in our system (Figure 6A). Another widely represented oxidatively modified proteins are the ones that facilitate protein degradation. Most of these are subunits of 26S proteasome, which is responsible for the removal of oxidatively damaged proteins in the cytosol and nucleus, and which itself was shown to be affected by oxidative stress.<sup>19</sup> Figure 6B refers only to carbonylated proteins classified by function. Clearly, functional distribution of carbonylated proteins differs from that of both carbonylated and oxidized thiol proteins (Figure 6, panels B and A, respectively). Remarkably, over 45% (55 out of 119) of carbonylated proteins are either structural proteins, chaperones or involved in energy metabolism. Table 1 summarizes proteins identified in our research that belong to families of structural or chaperone proteins and energy metabolism enzymes. Redox homeostasis and selected signaling proteins are listed in Table 2. Their possible roles in PDT-induced apoptosis will be discussed below.

**The Effect of PDT Depends on the Localization of the Photosensitizer.** In A431 cells the photosensitizer Pc4 was shown to bind selectively but not exclusively to mitochondria and other organelles, presumably Golgi complexes or endoplasmic reticulum (ER).<sup>20</sup> Classification of all identified proteins by cellular localization (Figure 6D) reveals that the majority of the affected proteins was cytosolic, whereas mitochondrial and ER proteins comprised about 20% of the total 314 oxidized proteins. Since nuclear localization of Pc4 was never shown, it was surprising that many nuclear proteins were identified in our approach. This can be explained by translocation of these proteins to the cytoplasm or by indirect oxidation, when nuclear proteins are modified not directly by ROS, but by another oxidized molecule, for example, a lipid. Remarkably, localization of carbonylated proteins (Figure 6E) significantly differs from that of oxidized thiol proteins (Figure 6F). Membrane proteins are enriched among carbonylated proteins, whereas nuclear proteins are underrepresented in this class of proteins. Since for protein carbonylation highly oxidizing conditions are required, these results might indicate that Pc4-induced oxidative stress is particularly strong in the cytoplasm, mitochondria, and in the hydrophobic environment of the membranes.

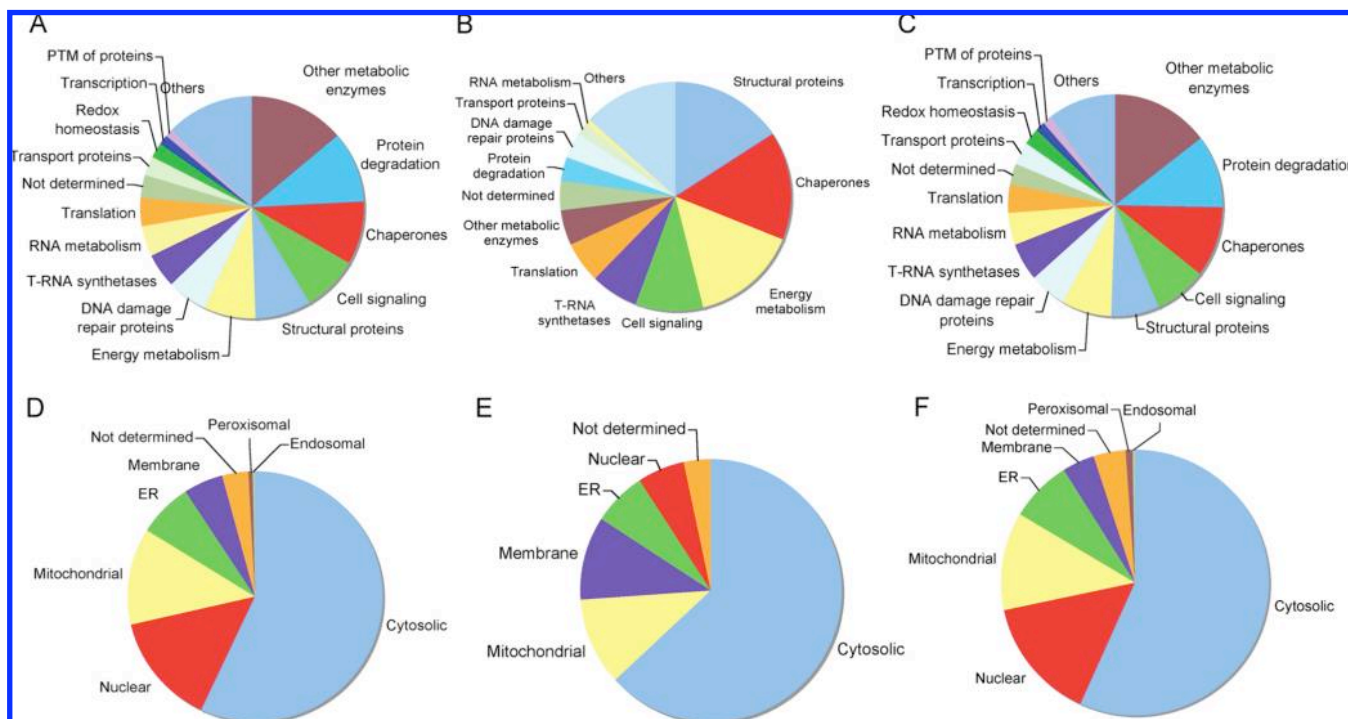


**Figure 6.** Functional classification of all 314 identified oxidatively modified proteins (A), of 119 carbonylated proteins (B) and of 281 thiol oxidized proteins (C). Classification by cellular localization of all oxidatively modified proteins (D), of carbonylated proteins (E) and of oxidized thiol proteins (F).

## Discussion

The importance of knowing signaling mechanisms that lead to activation of apoptotic cell death in PDT is widely acknowledged. Various apoptotic events induced by PDT have been observed, for example, cytochrome C release from mitochondria, loss of mitochondrial membrane potential, cleavage of various pro-caspases, PARP cleavage and DNA fragmentation.<sup>3</sup> PARP cleavage has been shown to occur early in the apoptotic progression as a result of the activity of caspase-3. PARP therefore may serve as a measure of apoptosis appearing as early as a few hours post the apoptosis-inducing event.<sup>21</sup> It makes PARP analysis a proper means for determination of working concentrations of photosensitizer. In our work, several different concentrations of Pc4 were tested. Figure 2A clearly shows that the photosensitizer Pc4 induces concentration-dependent PARP cleavage. Additionally, the percentage of cells undergoing apoptosis was estimated using fluorescence microscopy (Figure 2B). These effects correlate with previously published results of apoptosis induction in the same cells using a similar photosensitization system.<sup>22</sup> So far, the identity of immediate targets of oxidation by singlet oxygen produced by PDT remained obscure. It is clear, however, that proteins represent one of these targets. Furthermore, oxidation of proteins, as key molecules playing a role in many structural and functional aspects of living cells, might be involved in triggering or interfering with various pathways leading to apoptosis. In the present study, we apply a proteomic approach to investigate the protein oxidation in human cancer A431 cells induced by PDT with photosensitizer Pc4. This approach, schematically shown in Figure 1, combines recently developed techniques for biotinylation of reversibly oxidized cysteines<sup>13</sup> and for selective labeling of protein carbonyls with biotin hydrazide.<sup>12,14–16</sup> Biotinylation of oxidatively modified proteins allows their subsequent isolation from the crude cellular lysate

and identification by mass spectrometry, giving a significant advantage over DNPH and acetyl-tyramine-fluorescein probes that have been used to label oxidized proteins in previous studies of PDT-induced protein oxidation.<sup>8,23</sup> Moreover, simultaneous detection of protein carbonyl formation and oxidation of cysteines allows differentiation of proteins by the extent of their susceptibility to undergo oxidative modifications. One can also distinguish between reversibly oxidized proteins and proteins that are irreversibly modified and becoming substrates for degradation or aggregation. Some of the proteins that do not undergo carbonylation, but carry reversibly oxidized cysteine residues, might be candidates for being redox regulated under physiological conditions.

Application of our combined proteomic method to human epidermoid carcinoma A431 cells subjected to PDT with 1  $\mu$ M Pc4 has led to the identification of 314 proteins, including 33 carbonylated proteins, 195 proteins that carried exclusively oxidized cysteines, and 86 proteins containing both carbonyl groups and oxidized thiols. As expected, there were more oxidized thiol proteins than carbonylated proteins in the list of identified proteins, given that carbonyls are more difficult to induce than oxidation of cysteine residues.<sup>24</sup> Furthermore, over 70% of carbonylated proteins also carry oxidized cysteines.

**Untreated Cancer A431 Cells Contain Both Carbonylated and Oxidized Thiol Proteins.** In accordance with the observation that cancer, like many other age-related disorders, is accompanied by the accumulation of oxidatively modified proteins, we found 38 biotin hydrazide and 33 biotin maleimide labeled proteins in A431 cells not subjected to PDT (Figure 5A,B). In contrast to carbonylated proteins, the presence of oxidized thiol proteins in untreated samples might be explained not only by their physiological oxidized state, but also by incomplete blocking of reduced thiols with NEM during the labeling procedure. However, proteins like ER resident protein

**Table 1.** Summary of Oxidatively Modified Proteins Involved in Energy Metabolism and Belonging to Structural or Chaperones Protein Families

description	acc. no.	mass [Da]	no. matched peptides			
			oxidatively modified thiols		carbonylation	
			Pc4, 1 $\mu$ M	control	Pc4, 1 $\mu$ M	control
<b>Energy Metabolism</b>						
Alpha-enolase	IPI00465248	47152.2	25	11	6	0
Transketolase	IPI00643920	67861.4	17	9	4	0
Triosephosphate isomerase 1	IPI00465028	30772.8	14	4		
Fructose-bisphosphate aldolase A	IPI00465439	39402.6	16	3	11	4
Glyceraldehyde-3-phosphate dehydrogenase	IPI00219018	36035.3	10	4	5	3
Malate dehydrogenase, mitochondrial precursor	IPI00291006	35513.7	11	3	3	0
Glucose-6-phosphate isomerase	IPI00027497	63130.5	8	3	6	4
Phosphoglycerate kinase 1	IPI00169383	44597.3	12	0	3	3
Aconitate hydratase, mitochondrial precursor	IPI00017855	85410	10	0	6	3
Aspartate aminotransferase, cytoplasmic	IPI00219029	46230.1	6	0		
Aspartate aminotransferase, mitochondrial precursor	IPI00018206	47458.6	9	3	3	0
Transaldolase	IPI00744692	37523.7	7	0	3	0
Citrate synthase, mitochondrial precursor	IPI00025366	51695.7	8	3	3	0
Isoform Mitochondrial of Fumarate hydratase	IPI00296053	54619.8	5	0		
Pyruvate dehydrogenase E1 component subunit beta	IPI00003925	39215.4	6	0		
ATP-citrate synthase	IPI00021290	120824.8	4	0	4	3
6-phosphofructokinase type C	IPI00009790	85579.4	5	0		
6-phosphogluconate dehydrogenase, decarboxylating	IPI00219525	53123.9	3	0	4	0
Lactate dehydrogenase A	IPI00217966	36671.2			5	3
Pyruvate carboxylase, mitochondrial precursor	IPI00299402	129616.7			8	12
Isocitrate dehydrogenase [NADP] cytoplasmic	IPI00027223	46642.5			4	0
ATP synthase subunit alpha, mitochondrial precursor	IPI00440493	59734.1	10	0		
ATP synthase subunit beta, mitochondrial precursor	IPI00303476	56542.5	4	0	5	0
Isoform M2 of Pyruvate kinase isozymes M1/M2	IPI00479186	57919.5	12	0	5	4
<b>Structural Proteins</b>						
Actin, cytoplasmic 1	IPI00021439	41719.8	20	10	9	3
Filamin A, alpha	IPI00302592	279990.7	42	3	42	21
Isoform 1 of Filamin-B	IPI00289334	278171.9	17	0	27	5
Ezrin	IPI00843975	69396.6	27	3	6	0
Moesin	IPI00219365	67803.8	14	3	4	3
Radixin	IPI00017367	68547.5	6	0		
Ezrin-radixin-moesin-binding phosphoprotein 50	IPI00003527	38850.3	4	0		
Isoform 1 of Vinculin	IPI00291175	116706.3	23	0	6	0
Alpha-actinin-1	IPI00013508	103043.1	16	3	10	9
Alpha-actinin-4	IPI00013808	104839.2	4	0	4	0
Tubulin beta-2C chain	IPI00007752	49812.7	15	0	12	6
29 kDa protein (Tropomyosin 3)	IPI00178083	29061.4	11	0	4	0
Fascin	IPI00163187	54512.3	8	0	4	0
Microtubule-associated protein 4	IPI00396171	121002.5	4	0	4	0
Isoform 1 of Septin-9	IPI00784614	65384.3	7	0		
Isoform 1 of Myosin-Ib	IPI00376344	131972.7	5	0		
Plastin-2	IPI00010471	70274.1	14	3	4	0
Tubulin alpha-3 chain	IPI00180675	50117.7			6	0
Myosin-9	IPI00019502	226388.3			13	5
Talin-1	IPI00298994	269747.1			8	0
Isoform 1 of Kinectin	IPI00328753	156258.3			3	0
Kinesin heavy chain	IPI00012837	109668.3			3	0
Src substrate cortactin	IPI00029601	61743.7	18	0	4	0
PDZ and LIM domain protein 1	IPI00010414	36053.3	6	0		
Plastin 3	IPI00216694	70795.9	3	0		
<b>Chaperones</b>						
Isoform 1 of Heat shock cognate 71 kDa protein	IPI00003865	70881.8	29	8	11	5
Heat shock protein HSP 90-beta	IPI00414676	83249.3	26	4	16	11
Glucose-regulated protein 78 kDa	IPI00003362	72405.6	19	3	6	4
Stress-70 protein, mitochondrial precursor	IPI00007765	73663.3	18	3	5	3
Heat shock protein HSP 90-alpha 2	IPI00382470	98147.1	11	0	7	4
Heat shock 70 kDa protein 1B	IPI00807640	70036	12	0	5	3
Isoform Beta of Heat-shock protein 105 kDa	IPI00218993	92099	16	0	9	0
Heat shock 70 kDa protein 4	IPI00002966	94283	10	0	4	0
HSPD1 61 kDa protein	IPI00472102	61195.9	8	0	4	0
Protein disulfide-isomerase A3 precursor	IPI00025252	56766.6	31	7	9	7

Table 1. Continued

description	acc. no.	mass [Da]	no. matched peptides			
			oxidatively modified thiols		carbonylation	
			Pc4, 1 $\mu$ M	control	Pc4, 1 $\mu$ M	control
Protein disulfide-isomerase A4 precursor	IPI00009904	72916	21	3	5	0
Protein disulfide-isomerase precursor	IPI00010796	57100.1	15	3	4	0
Protein disulfide-isomerase A6 precursor	IPI00299571	53883.9	9	0		
Thioredoxin domain-containing protein 1	IPI00395887	31773.9	8	3		
Thioredoxin domain-containing protein 5	IPI00171438	47611.1	9	3		
T-complex protein 1 subunit 8	IPI00302925	59761.2	12	0	4	0
T-complex protein 1 subunit 3	IPI00290770	60446.3	9	0	3	0
T-complex protein 1 subunit beta	IPI00297779	57471.9	8	0		
T-complex protein 1 subunit eta	IPI00018465	59349.8	8	0	3	0
T-complex protein 1 subunit delta	IPI00302927	57908	9	0		
T-complex protein 1 subunit alpha	IPI00290566	60327.2	7	0	5	0
T-complex protein 1 subunit epsilon	IPI00010720	59654.3	3	0		
T-complex protein 1 subunit zeta	IPI00027626	58007.3	5	0		
150 kDa oxygen-regulated protein precursor	IPI00000877	111318.8	5	0		
Calnexin precursor	IPI00020984	67552.2	3	0		
Activator of 90 kDa heat shock protein	IPI00030706	38256.4	3	0	3	0
CDC37 Hsp90 cochaperone Cdc37	IPI00013122	44450.2	5	0		
Glucose-regulated protein 94 kDa	IPI00027230	92453.7	13	0	5	0
DnaJ homologue subfamily C member 10 precursor	IPI00293260	91064.4	3	0		

Table 2. Selected Oxidatively Modified Proteins Involved in Redox Homeostasis and Cell Signaling

description	acc. no.	mass [Da]	no. matched peptides			
			oxidatively modified thiols		carbonylation	
			Pc4, 1 $\mu$ M	control	Pc4, 1 $\mu$ M	control
<b>(A) Redox Homeostasis</b>						
Peroxiredoxin 1	IPI00000874	22092.9	13	3		
Peroxiredoxin-6	IPI00220301	25018.1	6	3		
Catalase	IPI00465436	59738.5	5	0		
Thioredoxin reductase 1	IPI00554786	54689.3	3	0		
Glutathione reductase	IPI00016862	56239.4	4	0		
Glutathione transferase omega-1	IPI00019755	27549.2	4	0		
Glutathione synthetase	IPI00010706	52367.9	3	0		
<b>(B) Cell Signaling</b>						
Epidermal growth factor receptor	IPI00018274	134261.2	20	3	20	6
Proliferation-associated protein 2G4	IPI00299000	43768.7	11	0	5	0
Isoform 1 of Nucleolin	IPI00604620	76597.9	19	0	5	0
Mitogen-activated protein kinase 3	IPI00018195	43119.4	3	0		
Serine/threonine-protein kinase PAK 2	IPI00419979	58059.2	3	0		
Cell cycle associated protein 1	IPI00150961	78346.4	3	0		
Serine/threonine-protein phosphatase 2A, alpha	IPI00554737	65291.7	4	0		
14-3-3 protein sigma	IPI00013890	27756.8	5	0		

disulfide-isomerase precursors, including thioredoxin domain-containing proteins 1 and 5, or ERO1-like  $\alpha$  protein that catalyze the rearrangement of disulfide bonds in proteins are known to contain oxidized cysteine residues under physiological conditions.<sup>25</sup> Interestingly, we also found the antioxidant proteins peroxiredoxins I and VI, that catalyze reduction of peroxides, to contain oxidized cysteines in cells that underwent no treatment. During the catalytic cycle, the redox-active Cys-52 of heterodimer Prx I is oxidized to Cys-52-SOH, which rapidly reacts with Cys-173 of the second subunit to form an intermolecular disulfide bond. Subsequently, the enzyme is regenerated by reduction of disulfide by Trx. In contrast, Prx VI contains only one conserved Cys-47 residue, which is involved in a catalytic cycle of peroxide-dependent oxidation (with the formation of Cys-47-SOH) and thiol-dependent reduction.<sup>26</sup> It has been shown that in the presence of glutathione S-transferase  $\pi$  Cys-47-SOH becomes glutathionylated (Cys-47-S-S-G), followed by the formation of disulfide between

Cys-47 of Prx VI and Cys-47 of GST  $\pi$ . Finally, the reduced active site Cys-47 of Prx VI is regenerated by GSH-mediated reduction of the disulfide. Each oxidized state of Cys-47 of Prx VI can be reduced by DTT and, consequently, detected by the method that we used. Thus, our results suggest that in A431 cells both Prx I and VI participate in the catalytic reduction of peroxides not only after oxidative treatment with Pc4 but also under physiological conditions.

**Susceptibility of Structural, Chaperone, and Energy Metabolism Proteins to Severe PDT-Induced Oxidation Accompanied by Carbonylation.** A recent study of carbonylated proteins in HL60 cells subjected to PDT with Pu-18, applying DNPH labeling of carbonyl groups, has revealed a specific set of oxidized proteins, including the structural proteins actin and tubulin, chaperones hsc71, Grp78, and PDI, and glycolytic enzyme  $\alpha$  enolase.<sup>8</sup> It has therefore been suggested that structural and chaperone protein families are the most susceptible to carbonylation and that their oxidation

could be an important event in the signaling pathway of apoptosis induced by PDT with Pu-18. In addition, application of the DNPH labeling method for studying protein carbonylation in HL60 cells undergoing apoptosis induced by VP16 treatment has led to the identification of Grp78 and actin, along with several glycolytic enzymes, that is,  $\alpha$  enolase, fructose bisphosphate aldolase, phosphoglycerate mutase, and triosephosphate isomerase.<sup>27</sup> Figure 6A–C shows the functional classification of all the proteins (314), carbonylated proteins (119) and thiols oxidized proteins (281) identified in our research. In agreement with previous studies,<sup>8,27</sup> the combined abundances of proteins that belong to families of structural proteins, chaperone proteins and energy metabolism enzymes differ strongly between carbonylated (Figure 6B) and oxidized thiol proteins (Figure 6C). Less than 25% (70 out of 281) of the proteins containing oxidized thiols and more than 45% (55 out of 119) of only carbonylated proteins belong to the three mentioned families. Thus, these proteins are enriched among the carbonylated proteins as compared to oxidized thiol proteins. Table 1 summarizes these proteins, many of which have been shown to undergo oxidative modifications induced by various stresses in different types of cells, for example,  $H_2O_2$  induced oxidation of GAPDH, moesin, heat shock protein 90  $\alpha$  and  $\beta$ , T-complex protein 1 subunit  $\alpha$ ;<sup>28</sup> alcohol induced oxidation of PDI A3 and A6 precursors;<sup>13</sup>  $H_2O_2$  induced oxidation of myosin, aconitase, ATP synthase  $\alpha$  and  $\beta$  subunits, malate and lactate dehydrogenases.<sup>29</sup>

The method used in this research is not quantitative. However, it has been shown that the number of peptides from each protein identified by MS/MS correlates with the amount of this protein.<sup>18</sup> As Table 1 indicates,  $\alpha$  enolase, fructose bisphosphate aldolase, actin, Hsc71, and Grp78 are among the proteins with the biggest number of matched peptides, irrespective of the type of oxidation. Assuming that these proteins are therefore abundant among the purified oxidatively modified proteins, it is logical that a poorly sensitive method, which uses DNPH labeling followed by mass spectrometry analysis of 2D-separated spots, has led to their identification.<sup>8,27</sup> Given that carbonyls are more difficult to induce than oxidatively modified thiols and that over 45% of identified carbonylated proteins are structural, chaperones or energy metabolism proteins, our results confirm that proteins from these three families are indeed largely susceptible to PDT-induced oxidation and usually undergo severe oxidation with the formation of both oxidative modifications. However, application of our sensitive method for purification of oxidized proteins allows identification of many more less abundant proteins or proteins that are less prone to oxidation (including low-abundance signaling proteins), giving a great advantage for understanding the mechanisms and the effects of PDT at the level of protein oxidation.

**PDT-Induced Oxidation of Redox Homeostasis Proteins.** For several proteins falling in the classes described above, reasonable evidence exists for their functional role in the cellular response to oxidative stress. We will speculate on the probable effects of oxidative modifications on the protein function and on the fate of the cell, emphasizing proteins involved in the cell cycle, cell signaling and apoptosis. The complete list of 314 proteins oxidized by PDT is presented in the Supplemental Table.

Several proteins involved in the maintenance of redox balance were found to become thiol oxidized by PDT (Table 2A). These include peroxiredoxins I and VI, catalase, thioredoxin

reductase 1, glutathione reductase, glutathione transferase omega 1 and glutathione synthetase. These proteins protect the cell from oxidative stress, for example, catalase converts hydrogen peroxide to oxygen and water, glutathione synthetase catalyzes the second step of the major cellular antioxidant GSH synthesis, and glutathione reductase maintains high levels of GSH in the cytosol. Oxidation of these proteins may affect their activity, decreasing the ability of the cell to resist oxidative stress and facilitating triggering and progression of PDT induced apoptosis.

**PDT-Induced Oxidation of Cdc37–Hsp90 Chaperone System.** We have identified several signaling proteins that undergo oxidative modifications in A431 cells subjected to PDT with Pc4. However, oxidation of two proteins that are not themselves signaling proteins requires special attention. These are Hsp90 and its co-chaperone Cdc37 which regulate activities of various proteins, mainly, kinases and transcription factors involved in cell cycle, growth, apoptosis and cancer signaling, for example, Akt, Cdk2, Cdk4, ErbB2, MEK1, Raf-1, p53, and many others.<sup>30</sup> Hsp90 is currently one of the hottest anti-cancer targets, since its inhibition triggers apoptosis in many cancer cells. Cdc37 forms a complex with Hsp90 that interacts with kinases while activating them.<sup>31</sup> Although we could not identify the exact cysteine in Cdc37 that was oxidatively modified, we hypothesize that oxidation of Cdc37 may lead to conformational changes and subsequent disruption of its interaction with Hsp90 and kinases. Consequences of this disruption should partly or fully overlap with the effect of Hsp90 inhibition. Thus, oxidation of Cdc37 and Hsp90, which might lead to loss of their interaction and apoptosis, represents one of the potential mechanisms of PDT-induced apoptotic cell death. This statement is strengthened by our unpublished observation that the amount of Cdc37 co-immunoprecipitated with Hsp90 is strongly reduced after subjection of A431 cells to PDT with Pc4.

**PDT-Mediated Epidermal Growth Factor Receptor (EGFR) Oxidation.** As we have found, one of the proteins that undergo extensive PDT-induced oxidation with the formation of both carbonyl groups and oxidized thiols is epidermal growth factor receptor (Table 2B). Recent work has shown that subjection of A431 cells to PDT with Pc4 resulted in a time-dependent decrease in EGFR protein expression and inhibition of tyrosine phosphorylation of EGFR.<sup>32</sup> Given that inhibition of EGFR-tyrosine kinase is known to result in an apoptotic cell death, the authors conclude that EGFR inhibition-mediated signaling is a partial contributor to the PDT-induced apoptosis. Our findings suggest the molecular mechanisms of the effects described above: PDT-mediated oxidative stress induces both reversible and irreversible oxidation of EGFR, presumably affecting its structure and function by decreasing kinase activity, making EGFR a substrate for protein degradation, which consequently decreases its cellular levels.

**PDT-Induced Oxidation of Signaling Proteins.** Proliferation-associated protein 2G4 (Ebp1) and nucleolin (Table 2B) have recently been shown to contribute to the regulation of *bcl-2* expression in HL-60 cells.<sup>33</sup> It has been proposed that by forming a heterocomplex, these proteins protect *bcl-2* mRNA from degradation, thus, maintaining high levels of anti-apoptotic Bcl-2 protein. Furthermore, it has been demonstrated that treatment with taxol or okadaic acid perturbs complex formation and leads to downregulation of

*bcl-2* mRNA followed by induction of the apoptosis. Also, Srivastava and co-workers have shown that PDT causes a time-dependent decrease in Bcl-2 levels in A431 cells.<sup>22</sup> As Table 2B indicates, both Ebp1 and nucleolin undergo severe PDT-induced oxidation. Since oxidative modifications of proteins, especially when accompanied with carbonyl formation, usually leads to conformational changes and alteration of binding properties, we hypothesize that oxidation of Ebp1 and nucleolin in A431 may negatively affect their interaction with each other or *bcl-2* mRNA, leading to a decrease in Bcl-2 levels and triggering apoptosis as described above.

More recent research has shown that phosphorylated Ebp1 binds to nuclear Akt and promotes cell survival by preventing apoptotic DNA fragmentation.<sup>34</sup> Summarizing here, we conclude that oxidation of Ebp1 and nucleolin may represent one of the immediate events induced by PDT that may directly trigger apoptosis, contributing to the multiple pathways activated by PDT.

Mitogen-activated protein kinase 3 (MAPK3/ERK1) is a member of a classical MAPK pathway and one of the downstream kinases of MEKK1. While MEKK1 already belongs to the growing list of proteins redox regulated by site-specific S-glutathionylation,<sup>35</sup> MAPK3 has been shown for the first time here to undergo cysteine oxidation in response to oxidative stress induced by PDT (Table 2B). This result, together with the observations that activities of different MAPK kinases were partly or fully inhibited by PDT in other cells,<sup>3</sup> suggests that MAPK3 is a putative substrate of redox regulation. PDT-induced thiol oxidation of MAPK3 may potentially inhibit its catalytic activity, leading to the loss of its survival signaling, thus, facilitating apoptotic death of cancer cells.

In conclusion, our studies provided the identity of a number of proteins affected by PDT. It should be realized, however, that further studies will be needed to shed more light on the functional consequences of protein oxidation and the possible role of these proteins in apoptosis.

**Supporting Information Available:** Table containing 314 proteins oxidatively modified by PDT, with indication of molecular weights, accession numbers and numbers of unique peptides identified by mass spectrometry. This material is available free of charge via the Internet at <http://pubs.acs.org>.

## References

- Dougherty, T. J.; Gomer, C. J.; Henderson, B. W.; Jori, J.; Kessel, D.; Korbek, M.; Moan, J.; Peng, Q. Photodynamic therapy. *J. Natl. Cancer Inst.* **1998**, *90* (12), 889–905.
- Moor, A. C. E. Signaling pathways in cell death and survival after photodynamic therapy. *J. Photochem. Photobiol.* **2000**, *57*, 1–13.
- Almeida, R. D.; Manadas, B. J.; Carvalho, A. P.; Duarte, C. B. Intracellular signaling mechanisms in photodynamic therapy. *Biochim. Biophys. Acta* **2004**, *1704*, 59–86.
- Agostinis, P.; Buytaert, E.; Breyssens, H.; Hendrickx, N. Regulatory pathways in photodynamic therapy induced apoptosis. *Photochem. Photobiol. Sci.* **2004**, *3*, 721–729.
- Klatt, P.; Molina, E. P.; De Lacoba, M. G.; Padilla, C. A.; Martinez-Galisteo, E.; Barcena, J. A.; Lamas, S. Redox regulation of c-Jun DNA binding by reversible S-glutathionylation. *FASEB J.* **1999**, *13*, 1481–1490.
- Lee, S. R.; Kwon, K. S.; Kim, S. R.; Rhee, S. G. Reversible inactivation of protein-tyrosine phosphatase 1B in A431 cells stimulated with epidermal growth factor. *J. Biol. Chem.* **1998**, *273* (25), 15366–14372.
- Finkel, T. Redox-dependent signal transduction. *FEBS Lett.* **2000**, *476*, 52–54.
- Magi, B.; Ettore, A.; Liberatori, S.; Bini, L.; Andreassi, M.; Frosali, S.; Neri, P.; Pallini, V.; Di Stefano, A. Selectivity of protein carbonylation in the apoptotic response to oxidative stress associated with photodynamic therapy: a cell biochemical and proteomic investigation. *Cell Death Differ.* **2004**, *11*, 842–852.
- Saitoh, M.; Nishitoh, H.; Fujii, M.; Takeda, K.; Tobiume, K.; Sawada, Y.; Kawabata, M.; Miyazono, K.; Ichijo, H. Mammalian thioredoxin is a direct inhibitor of apoptosis signal-regulating kinase (ASK) 1. *EMBO J.* **1998**, *17* (9), 2596–2606.
- Gotoh, Y.; Cooper, J. A. Reactive oxygen species- and dimerization-induced activation of apoptosis signal-regulating kinase 1 in tumor necrosis factor- $\alpha$  signal transduction. *J. Biol. Chem.* **1998**, *273* (28), 17477–17482.
- Miller, J. D.; Baron, E. D.; Scull, H.; Hsia, A.; Berlin, J. C.; McCormick, T.; Colussi, V.; Kenney, M. E.; Copper, K. D.; Oleinick, N. L. Photodynamic therapy with the phthalocyanine photosensitizer Pc4: The case experience with preclinical mechanistic and early clinical-translational studies. *Toxicol. Appl. Pharmacol.* **2007**, *224*, 290–299.
- Yoo, B.-S.; Regnier, F. Proteomic analysis of carbonylated proteins in two-dimensional gel electrophoresis using avidin-fluorescein affinity staining. *Electrophoresis* **2004**, *25*, 1334–1341.
- Kim, B.; Hood, B.; Aragon, R.; Hardwick, J.; Conrads, T.; Veenstra, T.; Song, B. Increased oxidation and degradation of cytosolic proteins in alcohol-exposed mouse liver and hepatoma cells. *Proteomics* **2006**, *6*, 1250–1260.
- Mirzaei, H.; Regnier, F. Affinity chromatographic selection of carbonylated proteins followed by identification of oxidation sites using tandem mass spectrometry. *Anal. Chem.* **2005**, *77* (8), 2386–2392.
- Oh-Ishi, M.; Ueno, T.; Maeda, T. Proteomic method detects oxidatively induced protein carbonyls in muscles of a diabetes model otsuka long-evans tokushima fatty (OLETF) rat. *Free Radical Biol. Med.* **2003**, *34* (1), 11–22.
- Ishii, T.; Sakurai, T.; Usami, H.; Uchida, K. Oxidative modification of proteasome: identification of an oxidation-sensitive subunit in 26S proteasome. *Biochemistry* **2005**, *44*, 13893–13901.
- Baty, J.; Hampton, M.; Winterbourn, C. Detection of oxidant sensitive thiol proteins by fluorescence labeling and two-dimensional electrophoresis. *Proteomics* **2002**, *2*, 1261–1266.
- Zybailov, B.; Coleman, M.; Florens, L.; Washburn, M. Correlation of relative abundance ratios derived from peptide ion chromatograms and spectrum counting for quantitative proteomic analysis using stable isotope labeling. *Anal. Chem.* **2005**, *77*, 6218–6224.
- Bader, N.; Grune, T. Protein oxidation and proteolysis. *Biol. Chem.* **2006**, *387*, 1351–1355.
- Lam, M.; Oleinick, N.; Nieminen, A. Photodynamic therapy induced apoptosis in epidermoid carcinoma cells. *J. Biol. Chem.* **2001**, *276*, 47379–47386.
- Perry, D.; Smyth, M.; Wang, H.; Reed, J.; Duriez, P.; Poirier, G.; Obeid, L.; Hannun, Y. Bcl-2 acts upstream of the PARP protease and prevents its activation. *Cell Death Differ.* **1997**, *4* (1), 29–33.
- Srivastava, M.; Ahmad, N.; Gupta, S.; Mukhtar, H. Involvement of Bcl-2 and Bax in photodynamic therapy-mediated apoptosis. Antisense Bcl-2 oligonucleotide sensitizes RIF 1 cells to photodynamic therapy apoptosis. *J. Biol. Chem.* **2001**, *276*, 15481–15488.
- Sakharov, D.; Bunschoten, A.; van Weelden, H.; Wirtz, K. Photodynamic treatment and H<sub>2</sub>O<sub>2</sub>-induced oxidative stress result in different patterns of cellular protein oxidation. *Eur. J. Biochem.* **2003**, *270*, 4859–4865.
- Shacter, E. Quantification and significance of protein oxidation in biological samples. *Drug Metab. Rev.* **2000**, *32*, 307–326.
- Benham, A.; Cabibbo, A.; Fassio, A.; Bulleid, N.; Sitia, R.; Braakman, I. The CXXCXXC motif determines the folding, structure and stability of human Ero1-La. *EMBO J.* **2000**, *19*, 4493–4502.
- Rhee, S.; Chae, H.; Kin, K. Peroxiredoxins: A historical overview and speculative preview of novel mechanisms and emerging concepts in cell signaling. *Free Radical Biol. Med.* **2005**, *38*, 1543–1552.
- England, K.; O'Driscoll, C.; Cotter, T. Carbonylation of glycolytic proteins is a key response to drug-induced oxidative stress and apoptosis. *Cell Death Differ.* **2004**, *11*, 252–260.
- Baty, J.; Hampton, M.; Winterbourn, C. Proteomic detection of hydrogen peroxide-sensitive thiol proteins in Jurkat cells. *Biochem. J.* **2005**, *389*, 785–795.
- Saurin, A.; Neubert, H.; Brennan, J.; Eaton, P. Widespread sulfenic acid formation in tissues in response to hydrogen peroxide. *Proc. Natl. Acad. Sci. U.S.A.* **2004**, *101*, 17982–17987.
- Pearl, L. Hsp90 and Cdc37 - a chaperone cancer conspiracy. *Curr. Opin. Genet. Dev.* **2005**, *15*, 55–61.

- (31) Voughan, C.; Gohlke, U.; Sobott, F.; Good, V.; Ali, M.; Prodromou, C.; Robinson, C.; Saibil, H.; Pearl, L. Structure of an Hsp90-Cdc37-Cdk4 complex. *Mol. Cell* **2006**, *23*, 697–707.
- (32) Ahmad, N.; Kalka, K.; Mukhtar, H. In vitro and in vivo inhibition of epidermal growth factor receptor-tyrosine kinase pathway by photodynamic therapy. *Oncogene* **2001**, *20*, 2314–2317.
- (33) Bose, S.; Sengupta, T.; Bandyopadhyay, S.; Spicer, E. Identification of Ebp1 as a component of cytoplasmic *bcl-2* mRNP (messenger ribonucleoprotein particle) complexes. *Biochem. J.* **2006**, *396*, 99–107.
- (34) Liu, Z.; Liu, X.; Nakayama, K.; Nakayama, K.; Ye, K. Protein kinase C- $\delta$  phosphorylates Ebp1 and prevents its proteolytic degradation, enhancing cell survival. *J. Neurochem.* **2007**, *100*, 1278–1288.
- (35) Cross, J.; Templeton, D. Oxidative stress inhibits MEKK1 by site-specific glutathionylation in the ATP binding domain. *Biochem. J.* **2004**, *381*, 697–707.

PR800189Q